Synthesis of C4-Linked C_0- and C_2-Imidazole 2′-Deoxyribonucleoside Phosphoramidites and Imidazole Base-Pairing Effects on DNA

Shinya Harusawa,*[a] Hiroki Yoneyama,[a] Yoshihide Usami,[a] Daisuke Yamamoto,[b] Zheng-yun Zhao[c]

[a] Laboratory of Pharmaceutical Organic Chemistry, Osaka University of Pharmaceutical Sciences, 4-20-1 Nasahara, Takatsuki, Osaka 569-1094, Japan
Fax +81(72)6901086; E-mail: harusawa@gly.oups.ac.jp

[b] Biomedical Computation Center, Osaka Medical College, 2-7 Daigakucho, Takatsuki, Osaka 569-8686, Japan

[c] Centre for Plant Science & Bio-polymer Research, Faculty of Engineering, Computing and Creative Industries, Edinburgh Napier University, 10 Colinton Road, Edinburgh, EH10 5DT, UK

Received: 20.05.2014; Accepted after revision: 17.06.2014

Abstract: The synthesis of C4-linked imidazole C_0- and C_2-2′-deoxyribonucleoside phosphoramidites (dPAs), in which the final phosphitylations are greatly improved by 4,5-dicyanoimidazole-promoted conversion, is described. The respective dPAs are successfully incorporated into the sequence of a 15-nt DNA, and the abilities of one or two imidazoles to pair with different bases are investigated through thermal melting (T_m) experiments on the resulting DNA duplexes. Furthermore, computational models of the imidazole-modified DNAs are found to be in good agreement with the results of the thermal melting experiments.

Key words: imidazole, phosphoramidite, C-deoxyribonucleoside, base pairing, DNA

Imidazole is present in many important biological molecules,[1] the most pervasive of which are histidine and histamine. The former plays a vital role in many proteins and enzymes,[2] while the latter is an endogenous biogenic amine having a number of pathophysiological roles.[3] Furthermore, imidazole is present in many pharmaceuticals such as fungicides and antifungal, antiprotozoal and antihypertensive medications.[4]

Imidazole, with a pK_a of 7.1, is employed extensively as a building block or as a Brønsted acid and base catalyst in organic chemistry.[1] However, imidazole-based compounds have not fulfilled important roles as chemical probes in nucleic acid chemistry, because to date there are few imidazole-intercalating agents.[5] From this viewpoint, we previously reported the efficient synthesis of C4-linked C_0- to C_3-imidazole ribonucleoside phosphoramidites [Imz-C_n-PAs (**1a**–**d**)], as shown in Figure 1.[6] During the synthesis of these phosphoramidites (PAs), pivaloyloxymethyl (POM)[6a,b] and cyanoethyl (CE)[6c] groups were employed successfully as protecting groups for the imidazole τ-nitrogen and 2′-hydroxy functions, respectively. Using Imz-C_n-PAs **1**,[6d] we have developed a novel chemogenetic approach in the studies of the catalytic mechanism of Varkud satellite (VS) and hairpin ribozymes,[7,8] where conventional nucleobases were replaced by imidazole as a powerful tool to probe general acid–base catalysis in the active sites of ribozymes.[6c,8] Evidence from this approach indicated that the chemical mechanisms of VS and hairpin ribozymes involve general acid–base catalysis via the combination of the specific adenine (A) and guanine (G) nucleobases (e.g., A756 and G638 in the VS ribozyme).[8] Of particular interest is that the modified VS ribozyme (G638C_2Imz), which is obtained from a two-carbon-elongated homologue [Imz-C_2-PA (**1c**)], shows significantly greater catalytic activity than G638C_0Imz, suggesting that the flexible C_2-methylene spacer is a better structural mimic of the purine nucleobase.[6c] In addition, starting from tetrazol(Tez)-C_0- and -C_2-PAs **2a** and **2b**, C5-linked C_0- and C_2-tetrazoles were incorporated successfully into the VS ribozyme substrate to determine more specifically which nucleobases of the ribozymes function as the acid or base.[9] Ribose-$(CH_2)_n$-Imz or -Tez species can, in principle, be incorporated at any site of RNA sequences through chemical synthesis.[10] Functional DNA oligonucleotides, in which a modified nucleobase bearing an alkylimidazole[11] or an imidazole N-deoxyribonucleoside[5] was incorporated, have already been reported. However, to the best of our knowledge, modified oligonucleotides substituted with an imidazole C-deoxyribonucleoside are not yet known.[12,13] Therefore, if C4-linked Imz-C_n-PAs based on 2′-deoxyribonucleosides could be synthesised, as an extension of the diversification of ongoing heterocyclic phosphoramidite synthesis in our group, they would greatly facilitate the chemogenetic approach to the investigation of various DNA functions. From systematic studies, we herein report the practical synthesis of Imz-C_0-2′-deoxyribonucleoside phosphoramidite (Imz-C_0-dPA) (**3a**) and the elongated novel C_2-homologue (Imz-C_2-dPA) (**3b**) as a purine base mimic (Figure 2, A). Phosphoramidites **3a** and **3b** were incorporated successfully into the centre of a 15-nt DNA sequence, and the abilities of the imidazole pairing with different bases were investigated by measuring the melting temperature (T_m) of the formed duplexes (Figure 2, B). Alternatively, two imidazole moieties were incorporated into the same sequence (Figure 2, B). Furthermore, Amber (*A*ssisted *m*odel *b*uilding with *e*nergy *r*efinement) models of their imidazole-incorporated DNA duplexes were constructed to interpret the results of the T_m experiments.

SYNTHESIS 2014, 46, 2815–2825
Advanced online publication: 31.07.2014
DOI: 10.1055/s-0034-1378451; Art ID: ss-2014-f0308-op

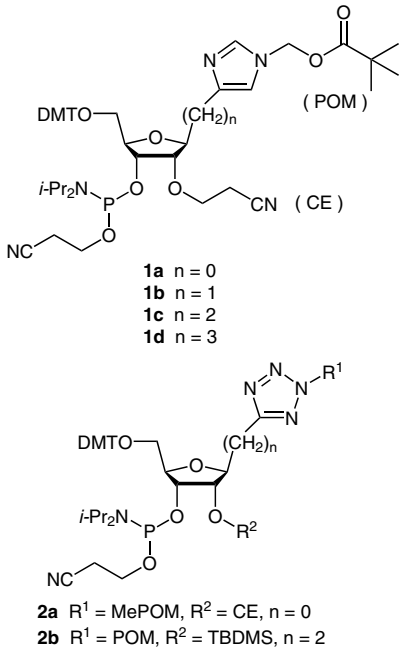

Figure 1 Structures of C4-linked imidazole- and C5-linked tetrazole-C$_n$-ribonucleoside phosphoramidites employed for solid-phase RNA synthesis

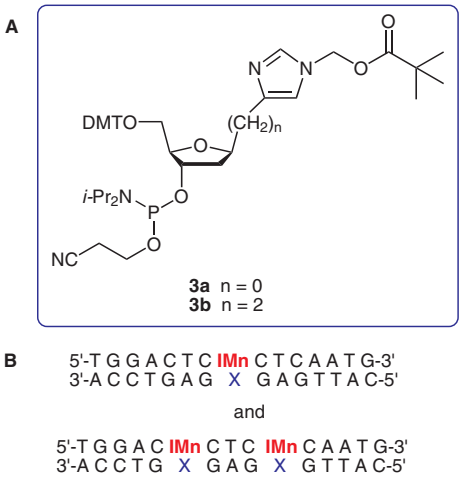

Figure 2 (A) Structures of imidazole-C$_n$-2′-deoxyribonucleoside phosphoramidites used for solid-phase DNA synthesis. (B) DNA duplexes containing one imidazole (IM) modification at the centre, and two IM modifications separated by three bases. **IMn** = IM (n = 0, from **3a**) or IM2 (n = 2, from **3b**; imidazole with a C2-linker). **X** = A, G, C, T, IM, IM2 or Ab (Abasic)

Modified Synthesis of Imz-C$_0$-dPA (3a)

We previously reported the synthesis of Imz-C$_0$-dPA (**3a**)[6b] from 4(5)-(3,5-di-*O*-benzyl-2′-deoxy-β-D-ribofuranosyl)-1*H*-imidazole (**4**),[13b] involving the introduction of a pivaloyloxymethyl group at the ^{im}N position of **4** (3 h, 90%), debenzylation of **5** to give **6** (3 h), dimethoxy (DM) tritylation of diol **6** yielding **7** [overnight, 51% from **5** (2 steps)], and phosphitylation of the 3′-hydroxy compound **7** (46 h, 14–32%), as shown in Scheme 1 (the percentage yields and reaction times in brackets show the results of the previous synthesis).[6b] Unfortunately, there was a serious limitation during the final step. The phosphitylation of **7** with 2-cyanoethyl *N*,*N*,*N*′,*N*′-tetraisopropylphosphoramidite (CETIP-PA) in the presence of diisopropylammonium tetrazolide (DIPT)[14a] proceeded slowly (46 h) in 1,2-dichloroethane (DCE) at 40 °C, and as a result, Imz-C$_0$-dPA (**3a**) was formed in 14–32% yields at most (Table 1, entry 1). Moreover, the isolation of **3a** from the reaction mixture was troublesome owing to the presence of by-products with similar polarities, resulting in low and variable yields. Significant effort was made to improve the reaction conditions, and additional experiments for the phosphitylation step were carried out in the present study. It was found that a shorter reaction time (22 h) provided **3a** (48%) with recovery of **7** (23%) (Table 1, entry 2), but a prolonged reaction (>22 h) resulted in generation of the by-products. Further, the phosphitylation of **7** using the alternative reagent, 2-cyanoethyl *N*,*N*-diisopropylchlorophosphoramidite, in the presence of *N*,*N*-diisopropylethylamine (DIPEA) proceeded smoothly at room temperature in one hour, but column chromatographic purification of the crude reaction mixture was not easy owing to the hydrolysed excess of the phosphitylating reagent, affording a moderate yield of **3a** (63%) (Table 1, entry 3). On the other hand, although diisopropylammonium tetrazolide is used as a common reagent in the P(III)–N activation strategy, 4,5-dicyanoimidazole (DCI) is an alternative to tetrazole-based activators.[14b] It is less acidic (pK_a = 5.2), but more nucleophilic than tetrazole (pK_a = 4.8) and its derivatives. Thus, when the 3′-hydroxy function of compound **7** was subjected to CETIP-PA (2 equiv) in the presence of 4,5-dicyanoimidazole (1.2 equiv) at 40 °C in 1,2-dichloroethane, the reaction proceeded cleanly to produce **3a** (94%) in only one hour (Table 1, entry 4). The crude product could be purified easily by column chromatography on basic silica gel to yield **3a** as a white foam, in contrast to the more time-consuming purification of the previous reaction[6b] using diisopropylammonium tetrazolide (Table 1, entry 1). In addition, although the previously reported debenzylation of **5** (reflux, 3 h) afforded diol **6** in moderate yield (<51%),[6b] the present reaction was completed quantitatively in only 30 minutes under microwave (MW) activation (Scheme 1).[9] Accordingly, the overall yield of Imz-C$_0$-dPA (**3a**) in the present synthetic study was 85% from deoxyribonucleoside **4**, which is a 6- to 13-fold increase compared to the aforementioned procedure, while the overall reaction time was reduced 17-fold.

Synthesis of Imz-C$_2$-dPA (3b)

Starting from 3,5-di-*O*-benzyl-1-cyano-2-deoxy-β-D-ribose (**8**),[15] the selective synthesis of β-aldehyde **9**[16] was carried out in two steps: treatment with a base followed by diisobutylaluminum hydride (DIBAL-H) reduction to yield the aldehyde (Scheme 2).[6c] The Wittig reaction of aldehyde **9** with *N*-1-trityl-4-imidazolylmethylphosphonium chloride (**10**)[6c] in toluene (–14 °C to r.t.) afforded the *E*-alkene product **11** (40%) and the corresponding *Z*-iso-

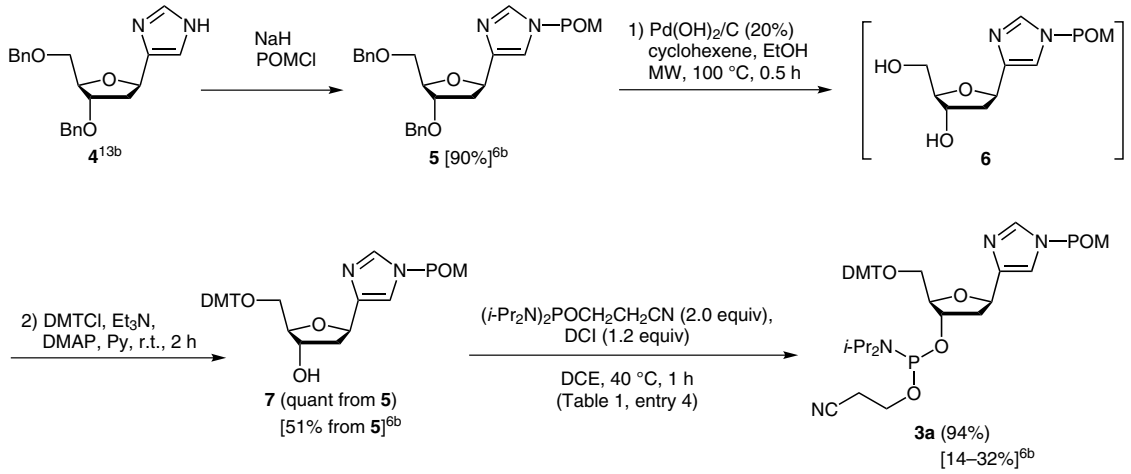

Scheme 1 Modified synthesis of Imz-C_0-dPA (**3a**) promoted by 4,5-dicyanoimidazole

mer **11** (16%), which were separated easily by column chromatography, while in tetrahydrofuran (–78 °C to r.t.) there was little *E*/*Z* preference for the newly formed double bond [(*E*)-**11** (26%), (*Z*)-**11** (33%)]. Acid treatment of each isomer to remove the trityl group, followed by the introduction of a pivaloyloxymethyl group provided (*E*)-**12** (54%) and the (*Z*)-isomer **12** (82%). Using (*E*)-**12**, we attempted the synthesis of a constrained *E*-vinyl-C_2-PA, but debenzylation (Li naphthalenide, $AlCl_3$–anisole, or BCl_3) whilst retaining the double bond of (*E*)-**12** failed to afford the desired intermediate **14**. Reductive debenzylation[9c] of combined isomers (*E*/*Z*)-**12**, under microwave irradiation,[9] involving simultaneous saturation of the double bond followed by dimethoxytritylation afforded *N*-POM-imidazole-C_2-deoxyribonucleoside **13** (67%). Finally, treatment of **13** with CETIP-PA in the presence of 4,5-dicyanoimidazole again proceeded smoothly to afford Imz-C_2-dPA (**3b**) (96%) as a white foam. The ^{31}P NMR spectroscopic data of **3b** indicated a pair of phosphorus diastereoisomers at 147.9 ppm and 148.4 ppm ($CDCl_3$). Mass spectrometric analysis of **3b** was performed using a matrix system [triethanolamine–NaCl] on a fast atom bombardment mass spectrometer (FABMS) equipped with a double-focusing mass spectrometer, which was recently developed in our laboratories for various labile phosphoramidites.[17] This technique successfully revealed the sodium ion adduct of **3b** at *m*/*z* 851.4129, confirming the chemical formula as $C_{46}H_{61}N_4O_8PNa$.

Base Pairing Experiments on Imidazole-Containing Oligomers

For the assessment of the imidazole base-pairing abilities with various bases, oligonucleotides containing imidazole moieties were prepared via automated DNA synthesis from the standard phosphoramidites (dA, dG, dC and T) and imidazole deoxyribonucleoside phosphoramidites **3a** and **3b**. Two experiments were designed. Firstly, imidazole moieties were introduced at the centre of a 15-nt duplex to replace a thymine–adenine (T/A) base pair [Figure

Table 1 Investigation of the Phosphitylation Conditions for the Synthesis of Compound **3a**

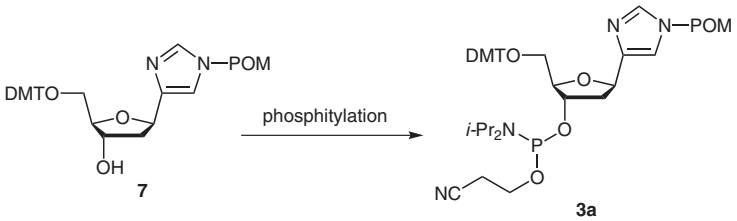

Entry	Conditions	Yield (%)
1	$(i\text{-}Pr_2N)_2POCH_2CH_2CN$ (1.1 equiv), DIPT[a] (0.5 equiv), 40 °C, 46 h, DCE	14–32[6b]
2	$(i\text{-}Pr_2N)_2POCH_2CH_2CN$ (1.1 equiv), DIPT (0.5 equiv), 40 °C, 22 h, DCE	48[c]
3	$i\text{-}Pr_2N(Cl)POCH_2CH_2CN$ (2.0 equiv), DIPEA (2.5 equiv), r.t., 1 h, CH_2Cl_2	63
4	$(i\text{-}Pr_2N)_2POCH_2CH_2CN$ (2.0 equiv), DCI[b] (1.2 equiv), 40 °C, 1 h, DCE	94

[a] DIPT = Diisopropylammonium tetrazolide.
[b] DCI = 4,5-Dicyano-1*H*-imidazole.
[c] Recovery of **7** (23%).

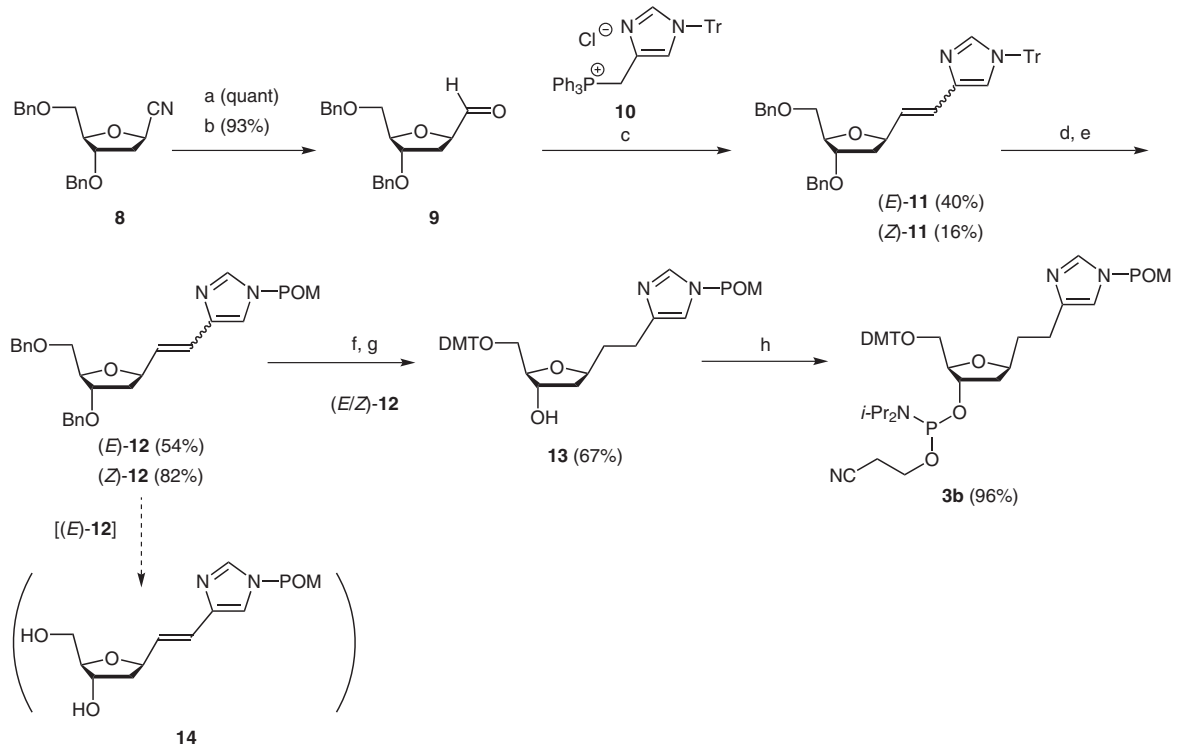

Scheme 2 Synthesis of Imz-C_2-dPA **3b**. *Reagents and conditions*: (a) NaOMe, MeOH, r.t., 15 h; (b) DIBAL-H, toluene, –78 °C, 0.5 h; (c) **10**, *n*-BuLi, toluene, –14 °C, then r.t., 2 h; (d) aq HCl, EtOH, reflux, 1 h; (e) NaH, POMCl, THF, r.t., 1 h; (f) 20% $Pd(OH)_2$/C, cyclohexene, EtOH, MW, 100 °C, 0.5 h; (g) DMTCl, Et_3N, DMAP (cat.), r.t., 2 h; (h) CETIP-PA, DCI, DCE, 40 °C, 1 h.

2 (B) and Table 2].[18] By varying the base directly opposite the imidazole in the probe strand, the impact from the base pairing could be assessed, while the two arms of the duplexes on each side with fully matched sequences could hold the duplexes together. Next, two thymines separated by three nucleobases were replaced by two imidazoles at centrally symmetric positions of the probe strand (Figure 2, B), and again, the opposite bases on the target strand were changed simultaneously to the same base, in the hope of obtaining further information. In both cases, the imidazole moieties only replaced the T bases in the probe strand. To assist the understanding of the interactions, we also prepared fully matched sequences with some modifications at the centre. These oligonucleotides were synthesised by solid-phase chemistry based on the phosphoramidite approach.[19] Stepwise coupling yield in over 99% were obtained for the phosphoramidites (Imz-dPAs) **3a** and **3b** as monitored from trityl release. All the prepared sequences are presented in Table 2. Details of the deprotection, purification, and analysis can be found in the Supporting Information. The thermal stability of each duplex was determined by variable temperature UV/Vis spectroscopy by monitoring the absorbance changes at 260 nm as a function of temperature. The melting temperature of a fully matched duplex with a T/A base pair in the centre was used as the control in each run of a set of experiments. The results are presented in Table 3. The following conclusions can be drawn:

(1) In the first row of Table 3, it is seen that imidazole (IM) pairs to a greater extent with purine bases (A or G) than with pyrimidine bases (C and T), possibly through hydrogen bonding. The fact that the same low T_m value (43.5 °C) was found for Abasic with Abasic (Ab, sugar moiety only) as for IM with IM (43.5 °C) indicates that there is little interaction between the IM moieties in the context of the duplex. In addition, IM with any base has a higher T_m (above 43.5 °C) indicating that there are indeed interactions between IM and the bases. However, all the modifications show lower T_m values than those of the fully matched T/A (56 °C) duplex.

(2) In the case of the imidazole with a C2 linker (IM2), there was not much difference observed in its pairing with different bases. IM2 paired with itself had a higher T_m of 48.5 °C. As we describe later, the modelling in the next section demonstrates some stacking interactions.

(3) When two IMs were introduced, as in the third row of Table 3, the T_m values show some additional effects. Again, it was found that IM interacts more strongly with purine bases than pyrimidine bases, consistent with the single IM substitution. However, two IM substitutions brought about more disruptions to duplex formation, hence lower T_m values were observed.

(4) With two IMs having C2 linkers incorporated into one strand, the corresponding duplexes showed pairing with A, G, and T, and afford almost the same T_m values, while pairing with cytosine (C) shows a higher value, however,

Table 2 Sequences of the Synthesised DNA Oligonucleotides

Oligonucleotide	Sequence (5′ to 3′)
Control probe	TGGACTCTCTCAATG
Control or A target	CATTGAGAGAGTCCA
IM probe[a]	TGGACTC**(IM)**CTCAATG
IM target	CATTGAG**(IM)**GAGTCCA
2IM probe	TGGAC**(IM)**CTC**(IM)**CAATG
IM2 probe	TGGACTC**(IM2)**CTCAATG
IM2 target[a]	CATTGAG**(IM2)**GAGTCCA
2IM2 probe	TGGAC**(IM2)**CTC**(IM2)**CAATG
Ab probe[b]	TGGACTC**(Ab)**CTCAATG
Ab target	CATTGAG**(Ab)**GAGTCCA
2Ab target	CATTG**(Ab)**GAG**(Ab)**GTCCA
G target	CATTGAG**G**GAGTCCA
C target	CATTGAG**C**GAGTCCA
T target	CATTGAG**T**GAGTCCA
2G target	CATTG**G**GAG**G**GTCCA
2C target	CATTG**C**GAG**C**GTCCA
2T target	CATTG**T**GAG**T**GTCCA

[a] IM or IM2 represents the imidazole (**3a**) or the imidazole with a C2 linker (**3b**) incorporated into the DNA sequence via phosphoramidite chemistry.
[b] **Ab** refers to Abasic, namely 2-deoxyribose without a base.

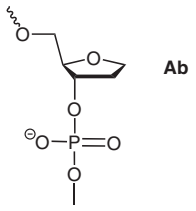

the reason for this is unclear. Perhaps, imidazole C2 linkers might be mimics of G. As it has been shown that C2-linked imidazole is similar structurally to a purine base, the N–H of imidazole would function similarly to G and would donate a proton to form an imino linkage for G/C pairs in the context of the DNA duplex. The fact that in all situations the T_m values were higher for all bases than with no bases, as in the case of Ab as a target, indicates that the imidazoles do indeed interact with bases.

Computational Models of Imidazole (IM/IM2)-Containing DNA

DNA duplex stability is a complicated issue, and might be affected by electrostatic, base stacking, and hydrophobic interactions, etc. Therefore, to understand the characteristic decrease in T_m values of modified DNA caused by the incorporation of IM or IM2, we compared four molecular

Table 3 Thermal Melting (T_m; °C) Data of the Duplexes Formed by Probes and Targets[a]

Probe \ Target	T/A control	A	G	C	T	Ab	Own (IMn)
IM	56	47	47	44	45	44	43.5
IM2	56	46	47.5	47.5	47	44.5	48.5
2IM	56	36.5	30.5	26.5	27.5	25	–
2IM2	56	32.5	34	37.5	33.5	32	–
Ab	–	–	–	–	–	43.5	–

[a] Reaction conditions: 5.0 μM of each oligonucleotide in NaCl (100 mM), phosphate (10 mM), and pH 7.0 buffer. IM and IM2 refer to **3a** and **3b** incorporated into sequences, and 2IM and 2IM2 refer to two identical modifications in a sequence. Likewise, in the target, for example, A stands for two As opposite the imidazole modifications in the target sequence with respect to 2IM and 2IM2. Ab refers to Abasic where there is no base, and only a sugar is present. Own refers to itself (i.e., the same modification pairing with itself in the centre of a sequence).

structures of the imidazole-modified duplexes with that of the fully-matched control duplex, as shown in Figure 3 (see the experimental section). The modelling indicated predicted duplex structures: the T–A control duplex (T_m = 56 °C), IM probe–A target (T_m = 47 °C), IM probe–IM target (T_m = 43.5 °C), IM2 probe–A target (T_m = 46 °C), and IM2 probe–IM2 target (T_m = 48.5 °C). In the control 15-nt DNA (Figure 3, A), two hydrogen bonds (3.39 Å and 2.87 Å) between T and A were present in the eighth base pair, and the aromatic rings of the eighth base pair were parallel-stacked between the seventh and ninth base pairs. Substitution of T with IM caused the breakdown of these hydrogen bonds (Figure 3, B), but the stacking interaction appeared to be maintained without distortion of the whole double-helix structure. In the case of the IM probe–IM target (Figure 3, C), there was a localised breakdown of the stacking interactions, and the imidazole rings of the IMs were fixed by hydrophobic interactions with the sugar moieties. In the IM2 probe–A target (Figure 3, D), an irregular hydrogen bond (2.86 Å) between IM2 and G adjacent to intrinsic A was formed, decreasing the regular stacking interaction of the control duplex. Finally, in the IM2 probe–IM2 target duplex (Figure 3, E), a hydrogen bond (2.84 Å) between the imidazole rings of the IM2 units and the regular stacking interaction were reconstructed in a similar way to those in the control duplex. These predicted molecular structures of IM/IM2-modified DNA duplexes are consistent with the decrease in the T_m values in each case.

The theoretical values of the interaction energies of the base pairs in these duplex structures are summarised in Table 4. The value for the eighth pair in each structure seemed to coincide with the above T_m values and the character of the molecular structure. From these results, we estimate the following order of stability: T–A > IM2–IM2 > IM2–A = IM–A > IM–IM. The values for the three base

pairs from the seventh to the ninth showed the same tendency, but the difference in the average per pair was small compared with that of the eighth pair. In terms of the interaction energy values for the five base pairs from the sixth to the tenth, the difference became smaller, and the duplex stability was out of order, except for that of IM–IM. Based on these findings, it was thought that the localised lack of stability brought about by IM/IM2 incorporation might be relieved by the molecular structure of the surrounding base pairs, especially by stacking interactions with the base ring moiety in the IM2–A and IM–A structures as described above. We postulated that this relieved stability was also shown in other base pair partial structures without hydrogen bonds, as is the case with a difluorotoluyl ribonucleoside in an RNA duplex structure.[20] Overall, the attack of water molecules on the localised unstable region might then spread along adjacent base pairs at a high temperature, similar to opening a zipper in both directions.

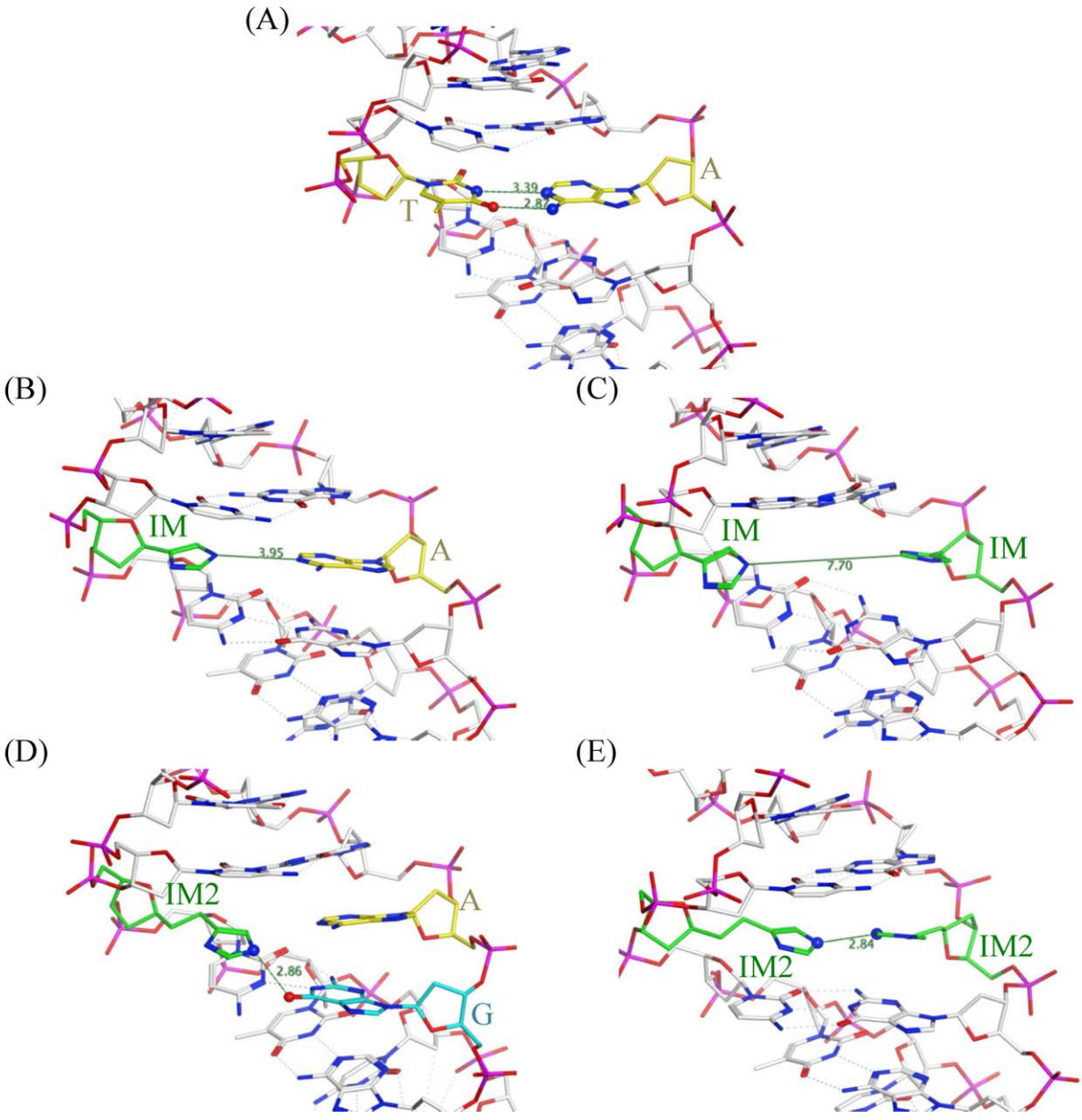

Figure 3 Predicted molecular structures of IM/IM2-incorporated DNA duplexes: (A) T–A control duplex; (B) IM probe–A target; (C) IM probe–IM target; (D) IM2 probe–A target; (E) IM2 probe–IM2 target. Oxygen, nitrogen, and phosphorus atoms are shown in red, blue and purple, respectively, and the carbon atoms of IM/IM2, the eighth nucleotide, G interacting with IM2(D) and other residues are shown in green, yellow, light blue, and white, respectively. Some interatomic distances related to the eighth residue are shown with green numbers, and the hydrogen bonds formed between atoms are shown as balls.

Table 4 Interaction Energies of Base Pairs in Imidazole-Substituted DNA Duplexes[a]

	Interaction energy (kcal/mol)		
8th Pair	8th Pair only	7–9th Pairs[b]	6–10th Pairs[b]
DNA (T–A)	–13.604	–88.446 (–29.482)	–133.161 (–26.632)
IM–A	–3.871	–80.99 (–26.999)	–138.303 (–27.661)
IM–IM	–0.311	–67.253 (–22.418)	–125.354 (–25.071)
IM2–A	–3.040	–79.488 (–26.496)	–136.365 (–27.273)
IM2–IM2	–9.357	–81.696 (–27.232)	–129.744 (–25.949)

[a] The theoretical values of the interaction energies (kcal/mol) of the 8th pair, 7–9th pairs, and 6–10th pairs in the control DNA duplex as well as the 8th-modified models (IM–A, IM–IM, IM2–A and IM2–IM2) are listed. These values were calculated using the MOE package under the same conditions of structural optimisation.
[b] Values in parentheses are the average values per pair.

In conclusion, a modified synthesis of C4-linked Imz-C_0-dPA (**3a**) was achieved via phosphitylation promoted by 4,5-dicyanoimidazole, significantly improving the overall yield and reaction times. Further, novel Imz-C_2-dPA (**3b**) as a purine base mimic was synthesised efficiently. By using phosphoramidites **3a** and **3b**, C_0- and C_2-imidazoles were incorporated, with over 99% stepwise coupling yields into the sequence of a 15-nt DNA, and the imidazole pairing abilities with different bases were examined through T_m experiments of the duplexes expressed as T_m values. These preliminary results indicated that: (i) duplexes containing C_0- or C_2-imidazole showed lower T_m values than the fully matched T/A control in all cases; (ii) a single imidazole paired with the purine bases (A and G) to a greater extent than with the pyrimidine bases (C and T); and (iii) pairing of the C_2-imidazole with nucleobases did not show much difference, but the pairing of C_2-imidazole with itself afforded higher T_m values. In addition, the results of the T_m experiments were in good agreement with those of the predicted models of imidazole-modified DNA duplexes. We see no reason why the synthesis of 2′-deoxyribonucleoside phosphoramidites **3a** and **3b** could not be scaled up to meet the needs of DNA studies, and therefore, **3a** and **3b** should be applicable for the insertion of C_n-imidazoles into DNA oligonucleotides. Further work on the applications of C_n-imidazole oligonucleotides is underway and the results will be reported in due course.

Reactions with air- and moisture-sensitive compounds were carried out under an Ar atmosphere. Microwave-assisted reactions were performed using a Milestone MultiSYNTH multimodal reactor with thermal control. Anhydrous solvents were purchased from WAKO Chemical Co. Solvents were dried over Na_2SO_4 and removed on a rotary evaporator under reduced pressure. Fuji Silysia FL-60D silica gel was used for flash column chromatography. Chromatorex NH-DM 1020 (Fuji Silysia Chemical Ltd.) was used for basic (NH) silica gel chromatography. TLC was performed on precoated TLC plates (Merck $60F_{254}$). ^{1}H (400 MHz) and ^{13}C NMR (100 MHz) spectra were recorded on an Agilent 400-MR-DD2 spectrometer in $CDCl_3$ with tetramethylsilane (TMS) as an internal standard. ^{31}P NMR spectra were recorded at 121 MHz on a Varian Mercury-300 spectrometer and the chemical shifts were measured relative to 85% H_3PO_4 as an external standard. High-resolution mass spectra were obtained using a JEOL JMS-700 mass spectrometer in positive-ion mode, with 3-nitrobenzyl alcohol (NBA) or triethanolamine (TEOA)/NaCl as the matrix.

[4-(5-*O*-DMT-2-deoxy-D-β-ribofuranosyl)imidazolyl]methyl 2,2-Dimethylpropionate (7)

A mixture of compound **5**[6b] (149 mg, 0.31 mmol), 20% $Pd(OH)_2$/C (90 mg) and cyclohexene (0.95 mL, 9.30 mmol) in EtOH was exposed to MW irradiation at 100 °C for 0.5 h. After filtration through Celite, the filtrate was evaporated to afford crude diol **6** as an oil, which was co-evaporated three times with pyridine (1 mL) and then dissolved in anhydrous pyridine (4 mL). DMTCl (159 mg, 0.47 mmol), Et_3N (64 μL, 0.47 mmol) and DMAP (4 mg, 0.03 mmol) were added to the pyridine solution, and the mixture was stirred at r.t. for 2 h. MeOH (1 mL) was added to the mixture which was then evaporated. The residue was subjected to chromatography on an NH-silica gel column (EtOAc) to afford **7**[6b] (190 mg, quant.) as an amorphous product.

[4-{5-*O*-DMT-2-deoxy-3-*O*-[2-cyanoethyl-(*N*,*N*-diisopropylamino)phosphoramidyl]-β-D-ribofuranos-1-yl}imidazolyl]methyl 2,2-Dimethylpropionate (3a)

Compound **7** (60 mg, 0.10 mmol) was dissolved in anhydrous DCE (3 mL), and DCI (14 mg, 0.12 mmol) and CETIP-PA (63 μL, 0.20 mmol) were added. The resulting mixture was stirred at 40 °C for 1 h and then evaporated. The residual oil was subjected to chromatography on NH-silica gel (EtOAc–hexane, 40:60 v/v) to afford **3a**[6b] (75 mg, 94%) as a white foam.

Synthesis of 3a Using 2-Cyanoethyl *N*,*N*-Diisopropylchlorophosphoramidite (Table 1, Entry 3)

DIPEA (85 μL, 0.50 mmol) and 2-cyanoethyl *N*,*N*-diisopropylchlorophosphoramidite (89 μL, 0.40 mmol) were added sequentially to compound **7** (120 mg, 0.20 mmol) in anhydrous CH_2Cl_2 (10 mL). After being stirred at r.t. for 1 h, the resulting mixture was diluted with CH_2Cl_2 (50 mL), and washed with sat. $NaHCO_3$ solution (30 mL) followed by H_2O (30 mL). The organic layer was dried over $MgSO_4$ and evaporated to afford a crude oil containing the hydrolysed phosphitylation reagent, which was chromatographed twice over NH-silica gel (EtOAc–hexane, 25:75 v/v) to afford **3a**[6b] (100 mg, 63%) as a white foam.

2-Deoxy-3,5-di-*O*-benzyl-β-D-ribofuranosylcarbaldehyde (9)

A mixture of NaOMe in MeOH (37.7 mL, 18.85 mmol, 0.5 M) and compound **8**[15] (4.06 g, 12.57 mmol) was stirred at r.t. for 15 h, and then acidified with aq HCl at 0 °C and evaporated to afford a residue, which was subsequently dissolved in EtOAc (100 mL). The organic layer was washed with H_2O (100 mL), dried and evaporated. The residue was purified by column chromatography on silica gel (EtOAc–hexane, 30:70 v/v) to afford methyl (2-deoxy-3,5-di-*O*-benzyl-β-D-ribofuranosyl)carboxylate (4.47 g, quant.) as an oil.

^{1}H NMR (400 MHz, $CDCl_3$): δ = 2.32–2.44 (m, 2 H), 3.54 (dd, *J* = 10.4, 4.4 Hz, 1 H), 3.56 (dd, *J* = 10.4, 4.4 Hz, 1 H), 3.70 (s, 3 H), 4.11 (quin, *J* = 2.8 Hz, 1 H), 4.38 (ddd, *J* = 4.4, 4.4, 2.8 Hz, 1 H), 4.45–4.57 (m, 4 H), 4.66 (dd, *J* = 8.0, 4.0 Hz, 1 H), 7.25–7.37 (m, 10 H).

^{13}C NMR (100 MHz, $CDCl_3$): δ = 35.9, 52.1, 70.2, 70.9, 73.4, 76.7, 79.5, 83.9, 127.5, 127.59, 127.62, 128.29, 128.34, 128.5, 137.8, 138.0, 173.4.

HRMS (FAB): *m*/*z* $[M + H]^+$ calcd for $C_{21}H_{25}O_5$: 357.1702; found: 357.1698.

DIBAL-H (4.0 mL, 4.0 mmol, 1 M solution in toluene) was added dropwise over a period of 10 min to a solution of the carboxylate (712 mg, 2.0 mmol) in toluene (10 mL) at –78 °C, and the mixture was stirred for 30 min at the same temperature. The reaction was quenched with MeOH (2 mL), and further stirred at r.t. Sat. $NaHCO_3$ solution (4 mL) and EtOAc (20 mL) were added and the mixture was stirred vigorously for 30 min. Anhydrous $MgSO_4$ was added to the resulting suspension, which was filtered through a Celite pad. The filtrate was evaporated and the residue was purified by column chromatography on silica gel (EtOAc–hexane, 1:3 v/v) to afford **9** (604 mg, 93%) as an oil.

^{1}H NMR (400 MHz, $CDCl_3$): δ = 2.24–2.34 (m, 2 H), 3.45 (dd, *J* = 10.4, 5.2 Hz, 1 H), 3.52 (dd, *J* = 10.4, 4.4 Hz, 1 H), 4.09 (ddd, *J* = 4.0, 2.4, 1.6 Hz, 1 H), 4.36–4.56 (m, 6 H), 7.23–7.38 (m, 10 H), 9.75 (d, *J* = 1.6 Hz, 1 H).

^{13}C NMR (100 MHz, $CDCl_3$): δ = 34.5, 70.60, 70.63, 73.5, 79.5, 82.8, 84.3, 127.5, 127.69, 127.73, 127.74, 128.4, 137.4, 137.8, 204.7.

HRMS (FAB): *m*/*z* [M + H]$^+$ calcd for $C_{20}H_{23}O_4$: 327.1596; found: 327.1601.

4-[(*Z*)-2-(2-Deoxy-3,5-di-*O*-benzyl-β-D-ribofuranos-1-yl)vinyl]-1-tritylimidazole [(*Z*)-11] and 4-[(*E*)-2-(2-Deoxy-3,5-di-*O*-benzyl-β-D-ribofuranos-1-yl)vinyl]-1-tritylimidazole [(*E*)-11]

n-BuLi (1.1 mL, 1.78 mmol, 1.6 M solution in hexane) was added dropwise over 10 min to a suspension of phosphonium salt **10** (1206 mg, 1.94 mmol) in THF (15 mL) at –78 °C, and the mixture was stirred for 30 min at the same temperature. A solution of aldehyde **9** (530 mg, 1.62 mmol) in THF (5 mL) was added dropwise over 10 min. After stirring for 2 h, the mixture was allowed to reach to r.t. and then quenched by the addition of H_2O. The mixture was evaporated and the residue was dissolved in EtOAc (100 mL). The organic layer was washed with H_2O (100 mL), dried and evaporated. The residue was purified by column chromatography on silica gel (EtOAc–hexane, 20:80 to 30:70 v/v) to afford the first fraction, (*Z*)-**11** (340 mg, 33%), as an oil, and the second fraction, (*E*)-**11** (270 mg, 26%), as an oil. When toluene was used as the solvent, the reaction was performed at –14 °C, affording (*E*)-**11** (40%) and (*Z*)-**11** (16%).

(*Z*)-11

^{1}H NMR (400 MHz, $CDCl_3$): δ = 1.88 (ddd, *J* = 12.8, 7.2, 5.6 Hz, 1 H), 2.50 (ddd, *J* = 12.8, 6.4, 6.4 Hz, 1 H), 3.45 (dd, *J* = 10.0, 5.2 Hz, 1 H), 3.50 (dd, *J* = 10.0, 5.2 Hz, 1 H), 4.11 (ddd, *J* = 6.4, 5.6, 4.0 Hz, 1 H), 4.25 (ddd, *J* = 5.2, 5.2, 4.0 Hz, 1 H), 4.45–4.54 (m, 4 H), 5.55 (ddd, *J* = 8.0, 7.2, 6.4 Hz, 1 H), 5.76 (dd, *J* = 11.6, 8.0 Hz, 1 H), 6.24 (d, *J* = 11.6 Hz, 1 H), 6.76 (d, *J* = 1.2 Hz, 1 H), 7.11–7.14 (m, 6 H), 7.23–7.33 (m, 19 H), 7.40 (d, *J* = 1.2 Hz, 1 H).

^{13}C NMR (100 MHz, $CDCl_3$): δ = 38.6, 70.8, 71.4, 73.3, 75.2, 75.4, 80.9, 82.2, 121.3, 121.4, 127.4, 127.47, 127.54, 127.6, 128.0, 128.2, 128.3, 129.7, 131.3, 138.21, 138.23, 138.3, 138.8, 142.2.

HRMS (FAB): *m*/*z* [M + H]$^+$ calcd for $C_{43}H_{41}N_2O_3$: 633.3118; found: 633.3113.

(*E*)-11

^{1}H NMR (400 MHz, $CDCl_3$): δ = 1.92 (ddd, *J* = 12.8, 7.2, 5.6 Hz, 1 H), 2.40 (ddd, *J* = 12.8, 6.4, 6.4 Hz, 1 H), 3.55 (d, *J* = 4.0 Hz, 2 H), 4.12–4.21 (m, 2 H), 4.45–4.65 (m, 5 H), 6.37 (dd, *J* = 16.0, 6.8 Hz, 1 H), 6.45 (d, *J* = 16.0 Hz, 1 H), 6.76 (s, 1 H), 7.10–7.16 (m, 6 H), 7.25–7.35 (m, 19 H), 7.39 (s, 1 H).

^{13}C NMR (100 MHz, $CDCl_3$): δ = 38.7, 70.7, 71.6, 73.4, 75.3, 79.3, 80.5, 82.1, 119.4, 123.1, 127.5, 127.56, 127.60, 127.7, 127.9, 128.0, 128.31, 128.32, 128.6, 129.7, 138.1, 138.3, 138.6, 139.0, 142.2.

HRMS (FAB): *m*/*z* [M + H]$^+$ calcd for $C_{43}H_{41}N_2O_3$: 633.3118; found: 633.3120.

{4-[(*Z*)-2-(2-Deoxy-3,5-di-*O*-benzyl-β-D-ribofuranos-1-yl)vinyl]imidazolyl}methyl 2,2-Dimethylpropionate [(*Z*)-12]

Aq 2 M HCl (5 mL) was added to a solution of (*Z*)-**11** (520 mg, 0.82 mmol) in EtOH (5 mL) and the mixture was heated at reflux temperature for 1 h. The mixture was cooled to r.t. and EtOAc (100 mL) was added. The resulting mixture was washed with sat. aq $NaHCO_3$ solution (50 mL), dried and evaporated. The residue was purified by column chromatography on silica gel (EtOAc) to afford 4-[(*Z*)-2-(2-deoxy-3,5-di-*O*-benzyl-β-D-ribofuranos-1-yl)vinyl]-1*H*-imidazole (290 mg, 91%) as an oil.

^{1}H NMR (400 MHz, $CDCl_3$): δ = 1.97 (ddd, *J* = 13.6, 8.0, 5.6 Hz, 1 H), 2.52 (ddd, *J* = 13.6, 6.8, 6.8 Hz, 1 H), 3.57 (dd, *J* = 10.4, 6.0 Hz, 1 H), 3.61 (dd, *J* = 10.4, 6.0 Hz, 1 H), 4.12 (ddd, *J* = 6.8, 5.6, 4.4 Hz, 1 H), 4.31 (ddd, *J* = 6.0, 4.4, 4.4 Hz, 1 H), 4.46–4.61 (m, 4 H), 4.92–4.96 (br s, 1 H), 5.64 (dd, *J* = 11.6, 6.0 Hz, 1 H), 6.43 (dd, *J* = 11.6, 1.6 Hz, 1 H), 7.00 (s, 1 H), 7.26–7.36 (m, 11 H).

^{13}C NMR (100 MHz, $CDCl_3$): δ = 38.9, 70.3, 71.7, 73.4, 74.9, 80.4, 82.0, 121.3, 127.60, 127.63, 127.7, 127.9, 128.37, 128.44, 136.1, 137.7, 137.8.

HRMS (FAB): *m*/*z* [M + H]$^+$ calcd for $C_{24}H_{27}N_2O_3$: 391.2021; found: 391.2013.

Under stirring, NaH (60 mg, 1.50 mmol, 60% in mineral oil) was added to THF (1 mL) to afford a suspension. A solution of the (*Z*)-vinylimidazole (390 mg, 1.00 mmol) in THF (4 mL) was added to the suspension and the resulting mixture was stirred at r.t. for 0.5 h. Next, chloromethyl pivaloate (0.22 mL, 1.50 mmol) was added. After 1 h, H_2O was added and the mixture was dissolved in EtOAc (100 mL). The organic layer was washed with H_2O (50 mL), dried and evaporated. The residue was purified by column chromatography on silica gel (EtOAc–hexane, 40:60 v/v) to afford (*Z*)-**12** (455 mg, 90%) as an oil.

^{1}H NMR (400 MHz, $CDCl_3$): δ = 1.16 (s, 9 H), 1.92 (ddd, *J* = 12.8, 7.6, 5.2 Hz, 1 H), 2.57 (ddd, *J* = 12.8, 6.4, 6.4 Hz, 1 H), 3.55 (dd, *J* = 10.4, 4.8 Hz, 1 H), 3.59 (dd, *J* = 10.4, 4.8 Hz, 1 H), 4.19 (ddd, *J* = 6.4, 5.2, 4.0 Hz, 1 H), 4.28 (ddd, *J* = 4.8, 4.8, 4.0 Hz, 1 H), 4.48–4.62 (m, 4 H), 5.46–5.52 (m, 1 H), 5.72 (d, *J* = 10.8 Hz, 1 H), 5.75 (d, *J* = 10.8 Hz, 1 H), 5.83 (dd, *J* = 11.6, 8.0 Hz, 1 H), 6.30 (d, *J* = 11.6 Hz, 1 H), 7.06 (d, *J* = 1.2 Hz, 1 H), 7.24–7.36 (m, 10 H), 7.60 (d, *J* = 1.2 Hz, 1 H).

^{13}C NMR (100 MHz, $CDCl_3$): δ = 26.8, 38.7, 67.6, 70.9, 71.5, 73.3, 75.4, 80.9, 82.3, 118.8, 121.6, 127.50, 127.54, 127.6, 128.30, 128.34, 132.0, 137.9, 138.2, 138.3, 139.9, 177.6.

HRMS (FAB): *m*/*z* [M + H]$^+$ calcd for $C_{30}H_{37}N_2O_5$: 505.2703; found: 505.2708.

{4-[(*E*)-2-(2-Deoxy-3,5-di-*O*-benzyl-β-D-ribofuranos-1-yl)vinyl]imidazolyl}methyl 2,2-Dimethylpropionate [(*E*)-12]

Aq 2 M HCl (5 mL) was added to a solution of (*E*)-**11** (470 mg, 0.74 mmol) in EtOH (5 mL) and the mixture was heated at reflux temperature for 1 h. The mixture was cooled to r.t. and EtOAc (100 mL) was added. The resulting mixture was washed with sat. aq $NaHCO_3$ solution (50 mL), dried and evaporated. The residue was purified by column chromatography on silica gel (EtOAc) to afford 4-[(*E*)-2-(2-deoxy-3,5-di-*O*-benzyl-β-D-ribofuranos-1-yl)vinyl]-1*H*-imidazole (234 mg, 81%) as an oil.

^{1}H NMR (400 MHz, $CDCl_3$): δ = 1.88 (ddd, *J* = 12.8, 7.2, 5.6 Hz, 1 H), 2.38 (ddd, *J* = 12.8, 6.4, 6.4 Hz, 1 H), 3.52 (dd, *J* = 10.4, 4.8 Hz, 1 H), 3.55 (dd, *J* = 10.4, 4.4 Hz, 1 H), 4.07–4.12 (m, 1 H), 4.17–4.24 (m, 1 H), 4.42–4.54 (m, 4 H), 4.60 (q, *J* = 7.2 Hz, 1 H), 6.22 (dd, *J* = 15.6, 7.2 Hz, 1 H), 6.43 (d, *J* = 15.6 Hz, 1 H), 6.88 (s, 1 H), 7.22–7.34 (m, 10 H), 7.44 (s, 1 H).

^{13}C NMR (100 MHz, $CDCl_3$): δ = 38.7, 70.8, 71.5, 73.4, 79.4, 80.4, 82.1, 121.4, 127.6, 127.9, 128.3, 135.7, 137.90, 137.92.

HRMS (FAB): *m*/*z* [M + H]$^+$ calcd for $C_{24}H_{27}N_2O_3$: 391.2021; found: 391.2020.

Under stirring, NaH (11 mg, 0.28 mmol, 60% in mineral oil) was added to THF (1 mL) to afford a suspension. A solution of the (*E*)-vinylimidazole (110 mg, 0.28 mmol) in THF (4 mL) was added to the suspension and the resulting mixture was stirred at r.t. for 0.5 h. Next, chloromethyl pivaloate (0.06 mL, 0.42 mmol) was added. After 1 h, H_2O was added and the mixture was dissolved in EtOAc (100 mL). The organic layer was washed with H_2O (50 mL), dried and evaporated. The residue was purified by column chromatography on silica gel (EtOAc–hexane, 50:50 v/v) to afford (*E*)-**12** (84 mg, 66%) as an oil.

^{1}H NMR (400 MHz, $CDCl_3$): δ = 1.16 (s, 9 H), 1.93 (ddd, *J* = 12.8, 7.2, 5.6 Hz, 1 H), 2.41 (ddd, *J* = 12.8, 6.4, 6.4 Hz, 1 H), 3.56 (d, *J* = 4.4 Hz, 1 H), 4.12–4.18 (m, 1 H), 4.22 (q, *J* = 4.4 Hz, 1 H), 4.46–4.68 (m, 5 H), 5.78 (s, 2 H), 6.43 (dd, *J* = 16.0, 4.8 Hz, 1 H), 6.48 (d, *J* = 16.0 Hz, 1 H), 6.98 (d, *J* = 1.2 Hz, 1 H), 7.25–7.35 (m, 10 H), 7.60 (d, *J* = 1.2 Hz, 1 H).

^{13}C NMR (100 MHz, $CDCl_3$): δ = 26.8, 38.7, 38.8, 67.6, 70.7, 71.6, 73.4, 79.1, 80.5, 82.2, 116.8, 122.2, 127.5, 127.56, 127.62, 127.7, 128.3, 128.4, 129.6, 138.2, 138.26, 138.31, 140.6, 177.7.

HRMS (FAB): *m*/*z* [M + H]$^+$ calcd for $C_{30}H_{37}N_2O_5$: 505.2703; found: 505.2705.

{4-[2-(5-*O*-DMT-2-deoxy-β-D-ribofuranos-1-yl)ethyl]imidazolyl}methyl 2,2-Dimethylpropionate (13)

A mixture of (*E*/*Z*)-**12** (270 mg, 0.53 mmol), 20% $Pd(OH)_2$/C (160 mg) and cyclohexene (1.6 mL, 15.9 mmol) in EtOH was exposed to MW irradiation at 100 °C for 0.5 h. After filtration through Celite, the filtrate was evaporated to afford {4-[2-(2-deoxy-β-D-ribofuranos-1-yl)ethyl]imidazolyl}methyl 2,2-dimethylpropionate (195 mg, quant.) as an oil.

^{1}H NMR (400 MHz, CD_3OD): δ = 1.18 (s, 9 H), 1.63 (ddd, *J* = 12.8, 6.8, 6.0 Hz, 1 H), 1.83–2.03 (m, 2 H), 2.34 (ddd, *J* = 12.8, 6.4, 6.4 Hz, 1 H), 2.66–2.83 (m, 2 H), 3.47–3.63 (m, 2 H), 3.78 (q, *J* = 4.8 Hz, 1 H), 4.00–4.10 (m, 1 H), 4.20 (q, *J* = 6.0 Hz, 1 H), 6.04 (s, 2 H), 7.37 (s, 1 H), 8.67 (s, 1 H).

^{13}C NMR (100 MHz, CD_3OD): δ = 23.3, 27.1, 36.1, 39.7, 41.3, 63.3, 70.3, 73.4, 78.4, 86.8, 118.9, 138.1, 138.7, 178.7.

HRMS (FAB): *m*/*z* [M + H]$^+$ calcd for $C_{16}H_{27}N_2O_5$: 327.1920; found: 327.1920.

The prepared diol (195 mg, 0.53 mmol) was co-evaporated three times with pyridine (1 mL) and dissolved in anhydrous pyridine (5 mL). DMTCl (271 mg, 0.80 mmol), Et_3N (110 μL, 0.80 mmol) and DMAP (6 mg, 0.05 mmol) were added to the solution, and the mixture was stirred at r.t. for 2 h. MeOH (1 mL) was added and the mixture was evaporated. The residue was subjected to chromatography on an NH-silica gel column (EtOAc) to afford compound **13** (224 mg, 67%) as an amorphous product.

^{1}H NMR (400 MHz, $CDCl_3$): δ = 1.16 (s, 9 H), 1.68 (ddd, *J* = 12.8, 7.2, 6.4 Hz, 1 H), 1.89–2.03 (m, 2 H), 2.34 (ddd, *J* = 12.8, 6.4, 6.4 Hz, 1 H), 2.55–2.75 (m, 2 H), 3.09 (dd, *J* = 9.6, 6.0 Hz, 1 H), 3.27 (dd, *J* = 9.6, 4.8 Hz, 1 H), 3.78 (s, 6 H), 3.98 (ddd, *J* = 6.0, 4.8, 4.8 Hz, 1 H), 4.06–4.14 (m, 1 H), 4.28 (td, *J* = 6.4, 4.8 Hz, 1 H), 5.71 (d, *J* = 11.6 Hz, 1 H), 5.73 (d, *J* = 11.6 Hz, 1 H), 6.78 (d, *J* = 1.2 Hz, 1 H), 6.80–6.84 (m, 4 H), 7.17–7.22 (m, 1 H), 7.25–7.34 (m, 6 H), 7.41–7.44 (m, 2 H), 7.54 (d, *J* = 1.2 Hz, 1 H).

^{13}C NMR (100 MHz, $CDCl_3$): δ = 24.6, 26.8, 35.7, 38.7, 40.2, 55.2, 64.8, 67.6, 74.8, 77.9, 83.5, 86.2, 113.1, 113.2, 115.4, 126.7, 127.8, 128.1, 129.99, 130.01, 135.97, 136.04, 137.4, 143.2, 144.8, 158.4, 177.6.

HRMS (FAB): *m*/*z* [M + H]$^+$ calcd for $C_{37}H_{45}N_2O_7$: 629.3227; found: 629.3224.

[4-(2-{5-*O*-DMT-2-deoxy-3-*O*-[2-cyanoethyl-(*N*,*N*-diisopropylamino)phosphoramidyl]-β-D-ribofuranos-1-yl}ethyl)imidazolyl]methyl 2,2-Dimethylpropionate (3b)

Compound **13** (63 mg, 0.10 mmol) was dissolved in anhydrous DCE (3 mL) and DCI (14 mg, 0.12 mmol) and CETIP-PA (63 μL, 0.20 mmol) were added. The resulting mixture was stirred at 40 °C for 1 h and then evaporated. The residual oil was subjected to chromatography on NH-silica gel (EtOAc–hexane, 40:60 v/v) to afford **3b** (80 mg, 96%) as two diastereomers (white foam).

^{1}H NMR (400 MHz, $CDCl_3$): δ = 0.99–1.06 (m, 2 H), 1.10–1.24 (m, 19 H), 1.72–1.85 (m, 1 H), 1.92–2.08 (m, 2 H), 2.32–2.44 (m, 2 H), 2.54–2.80 (m, 3 H), 3.06–3.13 (m, 1 H), 3.18–3.24 (m, 1 H), 3.48–3.62 (m, 3 H), 3.70–3.87 (m, 1 H), 3.78 (s, 3 H), 3.79 (s, 3 H), 4.10–4.22 (m, 2 H), 4.40–4.52 (m, 1 H), 5.69 (d, *J* = 10.8 Hz, 1 H), 5.73 (d, *J* = 10.8 Hz, 1 H), 6.79–6.83 (m, 5 H), 7.19–7.36 (m, 7 H), 7.43–7.47 (m, 2 H), 7.57 (d, *J* = 1.2 Hz, 1 H).

^{13}C NMR (100 MHz, $CDCl_3$): δ (diastereomeric mixture) = 20.0, 20.1, 20.2, 20.3, 21.5, 24.3, 24.4, 24.46, 24.53, 24.87, 24.91, 26.7, 35.37, 35.41, 38.6, 39.66, 39.70, 39.74, 42.9, 42.99, 43.03, 43.1, 55.1, 57.5, 58.0, 58.2, 64.0, 64.2, 67.6, 75.0, 75.2, 75.3, 75.5, 76.7, 78.3, 83.6, 83.67, 83.72, 85.8, 112.9, 115.3, 117.46, 117.54, 126.56, 126.61, 127.7, 128.16, 128.22, 130.0, 130.1, 136.08, 136.13, 137.5, 143.2, 144.9, 158.3, 177.6.

^{31}P NMR (121 MHz, $CDCl_3$): δ = 147.9, 148.4.

HRMS (FAB: TEOA + NaCl):[17] *m*/*z* [M + Na]$^+$ calcd for $C_{46}H_{61}N_4O_8PNa$: 851.4125; found: 851.4129.

Oligonucleotide Synthesis and Purification

Oligonucleotides were synthesised with trityl-OFF on a 1.0 μM scale on a controlled pore glass (CPG) solid support using a procedure based on phosphoramidite chemistry.[19] Commercially available DNA reagents and solvents were obtained from Links Technologies, Applied Biosystems and Ruthburn Ltd., respectively. The standard phosphoramidites (Bz-dA, ibu-dG, Ac-dC, and T) and prepared imidazole phosphoramidites were dissolved in anhydrous MeCN to a concentration of 0.1 M prior to the synthesis. Ethylthio-1*H*-tetrazole (ETT; 0.25 M) in MeCN was used as an activator and I_2/H_2O (0.02 M) was used as an oxidiser. A 1.0 μM DNA/RNA synthetic cycle involving acid detritylation, coupling, capping and oxidation steps was used. For IM modification, an extended coupling time of 10 min was used, while for standard bases, a coupling time of 25 s was used. The required sequences were cleaved from the solid support by treatment with concd aq NH_3 for approximately 1 h on the synthesiser. The solutions were then heated in a sealed vial at 55 °C for 6 h for deprotection before being concentrated on a Speedvac.

The residues were dissolved in H_2O (1.0 mL) and purified by reversed-phase HPLC on a C18 column (Phenomenex Clarity 5 μ Oligo-RP column, 150 × 10 mm), and eluted with 0.1 M TEAA (pH 7.0) and MeCN mixtures with a flow rate of 3.0 mL/min. The fractions of the major peak, monitored at 260 nm, were collected and evaporated. The residue was dissolved in H_2O and desalted by passing through an NAP-10 column (GE Healthcare) following the manufacturer's instructions.

The purity of each oligonucleotide was assessed by analytical HPLC and mass spectrometry. The analysis conditions and results for key oligonucleotides are presented in the Supporting Information.

UV/Vis spectra were recorded with a UV-1800 Shimadzu UV spectrophotometer. The concentrations of each oligonucleotide were determined by measuring the absorbance at 260 nm. The molar extinction coefficients of the oligonucleotides were obtained by submitting the sequences on the IDT UV spectrum website (http://biophysics.idtdna.com/UVSpectrum.html). The absorbance of imidazole compared with those of the nucleobases at 260 nm was negligible. The concentrations of these oligonucleotides were obtained in the range 150–300 μM as solutions in H_2O (1.5 mL).

T_m Measurements

A 5.0 μM solution of each oligonucleotide strand in 1.0 mL of a pH 7.0 buffer containing phosphate buffer (10 mM), and NaCl (100 mM) was prepared. The solution was heated at 80 °C for 5 min and then allowed to cool slowly to r.t. over a period of 4 h before being

placed in a UV spectrometer with temperature control for recording the T_m measurements.

Molecular Modelling of the DNA Duplex Model and IM/IM2 Incorporated Structures

A theoretical molecular model for the DNA duplex of 5′-TG-GACTCTCTCAATG-3′ (control probe) and 5′-CATTGAGA-GAGTCCA-3′ (control target) was constructed as a B-DNA form using the MOE (Molecular Operating Environment 2013.0801, Chemical Computing Group Inc., Québec, CA; http://www.chemcomp.com/) package for molecular structure analyses. The model was initially optimised by energy minimisation using the Amber12 EHT force field.[21] The energy cut-off distance was set at 10 Å, and the dielectric constant was distance-dependent, based on a value of 1.0 for the DNA molecule and 80.0 for the exterior space. Subsequently, a 500-ps molecular dynamics simulation was performed on the model at 300 K using a 0.002 ps time step, the same force field, and the NPA (Nosé–Poincaré–Anderson) Hamiltonian equations.[22] Before these equilibrium iterations, 5-ps heating iterations were employed to account for stable equilibration. Finally, the most stable structure during the latter 50-ps simulations was optimised by energy minimisation. Considering the molecular stability of the DNA molecule at 300 K (26.85 °C), atoms of four nucleotides of both termini were tethered in the space at 1.0 Å from those atomic positions in the initial B-DNA form during all the optimisation steps. Complex molecules of IM probe–A, IM probe–IM, IM2 probe–A, and IM2 probe–IM2 targets were modelled from the above B-DNA form, and these molecular models were also optimised through the above methods. All modelling operations, including calculations for the optimisation steps, were performed using MOE.

Acknowledgment

We thank Dr. M. Fujitake of Osaka University of Pharmaceutical Sciences for MS measurements. This work was supported in part by a Grant-in-Aid for Scientific Research [Grant No. 21590130 (S.H.)] from JSPS, 2009–2013. We thank the EPSRC, Advantage West Midlands, University of Birmingham and the analytical facility within the School of Chemistry for support.

Supporting Information for this article is available online at http://www.thieme-connect.com/products/ejournals/journal/10.1055/s-00000084.

References

(1) Grimmett, M. R. *Imidazoles*, In *Comprehensive Heterocyclic Chemistry II*; Vol. 3; Katritzky, A. R.; Rees, C. W.; Scriven, E. F. V., Eds.; Pergamon: Oxford, **1996**, 77.

(2) (a) Kopple, J. D.; Swendseid, M. E. *J. Clin. Invest.* **1975**, *55*, 881. (b) Fahey, R. C. *Annu. Rev. Microbiol.* **2001**, *55*, 333.

(3) (a) Marieb, E. N. In *Human Anatomy & Physiology*; Benjamin-Cummings: San Francisco, **2001**, 414, 796, 824 and 90. (b) Repka-Ramirez, M. S. *Curr. Allergy Rep.* **2003**, *30*, 227. (c) Hough, L. B. *Mol. Pharmacol.* **2001**, *59*, 415.

(4) (a) Madasu, S. B.; Vekariya, N. A.; Koteswaramma, C.; Islam, A.; Sanasi, P. D.; Korupolu, R. B. *Org. Process Res. Dev.* **2012**, *16*, 2025. (b) Walsh, A. J.; Davis, M. L.; Fraser, W. *Molecules* **2006**, *11*, 486. (c) Mangas-Sánchez, J.; Busto, E.; Gotor-Fernández, V.; Malpartida, F.; Gotor, V. *J. Org. Chem.* **2011**, *76*, 2115. (d) Liang, J.; Lv, W.; Li, X.; An, K.; Cushman, M.; Wang, H.; Xu, Y. *Bioorg. Med. Chem. Lett.* **2013**, *23*, 1387.

(5) For oligodeoxyribonucleotides containing an imidazole N-nucleoside, see: (a) Johannsen, S.; Megger, N.; Böhme, D.; Siegel, R. K. O.; Müller, J. *Nat. Chem.* **2010**, *2*, 229. (b) Durland, R. H.; Rao, T. S.; Bodepudi, V.; Seth, D. M.; Jayaraman, K.; Revankar, G. R. *Nucleic Acids Res.* **1995**, *23*, 647. (c) Johnson, W. T.; Zhang, P.; Bergstrom, D. E. *Nucleic Acid Res.* **1997**, *25*, 559.

(6) (a) Araki, L.; Harusawa, S.; Yamaguchi, M.; Yonezawa, S.; Taniguchi, N.; Lilley, D. M. J.; Zhao, Z.; Kurihara, T. *Tetrahedron Lett.* **2004**, *45*, 2657. (b) Araki, L.; Harusawa, S.; Yamaguchi, M.; Yonezawa, S.; Taniguchi, N.; Lilley, D. M. J.; Zhao, Z.; Kurihara, T. *Tetrahedron* **2005**, *61*, 11976. (c) Araki, L.; Morita, K.; Yamaguchi, M.; Zhao, Z.; Wilson, T. J.; Lilley, D. M. J.; Harusawa, S. *J. Org. Chem.* **2009**, *74*, 2350. (d) Araki, L.; Zhao, Z.; Lilley, D. M. J.; Harusawa, S. *Heterocycles* **2010**, *81*, 1861. (e) Harusawa, S.; Fujii, K.; Nishiura, M.; Araki, L.; Usami, Y.; Zhao, Z.; Lilley, D. M. J. *Heterocycles* **2011**, *83*, 2041. (f) Araki, L.; Harusawa, S. *Yakugaku Zasshi* **2010**, *130*, 1707.

(7) Lilley, D. M. J. *The Hairpin and Varkud Satellite Ribozymes*, In *Ribozymes and RNA Catalysis*; Lilley, D. M. J.; Eckstein, F., Eds.; Royal Society of Chemistry: Cambridge, **2008**, 66.

(8) (a) Zhao, Z.; McLeod, A.; Harusawa, S.; Araki, L.; Yamaguchi, M.; Kurihara, T.; Lilley, D. M. J. *J. Am. Chem. Soc.* **2005**, *127*, 5026. (b) Wilson, T. J.; Ouellet, J.; Zhao, Z.; Harusawa, S.; Araki, L.; Kurihara, T.; Lilley, D. M. J. *RNA* **2006**, *12*, 980. (c) Lilley, D. M. J. *Biol. Chem.* **2007**, *388*, 699.

(9) (a) Harusawa, S.; Yoneyama, H.; Fujisue, D.; Nishimura, M.; Fujitake, M.; Usami, Y.; Zhao, Z.; McPhee, S. A.; Wilson, T. J.; Lilley, D. M. J. *Tetrahedron Lett.* **2012**, *45*, 5891. (b) Yoneyama, H.; Usami, Y.; Komeda, S.; Harusawa, S. *Synthesis* **2013**, *45*, 1051. (c) The typical debenzylation of 3,5-di-*O*-benzyl-2-deoxy-β-D-riboses with $Pd(OH)_2$/C–cyclohexene in ethanol at reflux temperature proceeds slowly, giving moderate yields of the products.

(10) Li, Z.; Zhou, H.; Wu, X.; Yao, H. *Curr. Med. Chem.* **2013**, *20*, 3641.

(11) (a) Sakthivel, K.; Barbas, C. F. III *Angew. Chem. Int. Ed.* **1998**, *37*, 2872. (b) Lee, S. E.; Sidorov, A.; Gourlain, T.; Mignet, N.; Thorpe, S. J.; Brazier, J. A.; Dickman, M. J.; Hornby, D. P.; Grasby, J. A.; Williams, D. M. *Nucleic Acids Res.* **2001**, *29*, 1565. (c) Sawai, H.; Ozaki, A. N.; Satoh, F.; Ohbayashi, T.; Masud, M. M.; Ozaki, H. *Chem. Commun.* **2001**, 2604. (d) Perrin, D. M.; Garestier, T.; Hélène, C. *J. Am. Chem. Soc.* **2001**, *123*, 1556.

(12) For recent reviews on C-nucelosides, see: (a) Boutureira, O.; Matheu, M. I.; Díaz, Y.; Castillón, S. *Synthesis of C-Nucleosides*, In *Chemical Synthesis of Nucleoside Analogues*; Merino, P., Ed.; Wiley: Hoboken, **2013**, 263. (b) Wu, Q.; Simons, C. *Synthesis* **2004**, 1533. (c) Štambaský, J.; Hocek, M.; Kočovský, P. *Chem. Rev.* **2009**, *109*, 6729.

(13) For the synthesis of C4-linked imidazole 2′-deoxyribonucleosides, see: (a) Bergstrom, D. E.; Zhang, P.; Zhou, J. *J. Chem. Soc., Perkin Trans. 1* **1994**, 3029. (b) Harusawa, S.; Murai, Y.; Moriyama, H.; Imazu, T.; Ohishi, H.; Yoneda, R.; Kurihara, T. *J. Org. Chem.* **1996**, *61*, 4405.

(14) (a) Beaucage, S. L. *Oligodeoxyribonucleoside Synthesis*, In *Protocols for Oligonucleotides and Analogs*; Agrawal, S., Ed.; Humana Press: Totowa (NJ), **1993**, 33. (b) Vargeese, C.; Carter, J.; Yegge, J.; Krivjansky, S.; Settle, A.; Kropp, E.; Peterson, K.; Pieken, W. *Nucleic Acids Res.* **1998**, *26*, 1046.

(15) Seitz, G.; Lachmann, J. *Z. Naturforsch.* **1999**, *54b*, 549.

(16) (a) The synthesis of a C2-α/β mixture (**9αβ**) of a furancarbaldehyde was reported (see ref. 16b), but the selective synthesis of **9β** was first carried out in this paper. (b) Krishna, P. R.; Reddy, V. V. R.; Srinivas, R. *Tetrahedron* **2007**, *63*, 9871.

(17) (a) Fujitake, M.; Harusawa, S.; Araki, L.; Yamaguchi, M.; Lilley, D. M. J.; Zhao, Z.; Kurihara, T. *Tetrahedron* **2005**, *61*, 4689. (b) Harusawa, S.; Fujitake, M.; Kurihara, T.; Zhao, Z.; Lilley, D. M. J. *Mass Determination of Phosphoramidites*, In *Current Protocols in Nucleic Acid Chemistry*; Beaucage, S. L.; Bergstrom, D. E.; Herdewijn, P.; Matsuda, A., Eds.; John Wiley & Sons: New York, **2006**, 10.11.1. (c) Fujitake, M.; Harusawa, S. *Yakugaku Zasshi* **2013**, *133*, 823.

(18) Manchester, J.; Bassani, D. M.; Duprey, J.-L. H. A.; Giordano, L.; Vyle, J. S.; Zhao, Z.-y.; Tucker, J. H. R. *J. Am. Chem. Soc.* **2012**, *134*, 10791.

(19) Beaucage, S. L.; Caruthers, M. H. *Tetrahedron Lett.* **1981**, *22*, 1859.

(20) Xia, J.; Noronha, A.; Toudjarska, I.; Li, F.; Akinc, A.; Braich, R.; Frank-Kamenetsky, M.; Rajeev, K. G.; Egli, M.; Manoharan, M. *ACS Chem. Biol.* **2006**, *1*, 176.

(21) Salomon-Ferrer, R.; Case, D. A.; Walker, R. C. *WIREs Comput. Mol. Sci.* **2013**, *3*, 198.

(22) Sturgeon, J. B.; Laird, B. B. *J. Chem. Phys.* **2000**, *112*, 3474.